PCCP

PAPER

View Article Online
View Journal

Cite this: DOI: 10.1039/c9cp03730f

Insight into the hybrid luminescence showed by carbon dots and molecular fluorophores in solution†

Ricardo M. S. Sendão,[a] Diana M. A. Crista,[a] Ana Carolina P. Afonso,[a] Maria del Valle Martínez de Yuso,[b] Manuel Algarra,[c] Joaquim C. G. Esteves da Silva[ad] and Luís Pinto da Silva *[ad]

Received 2nd July 2019,
Accepted 9th September 2019

DOI: 10.1039/c9cp03730f

rsc.li/pccp

Carbon dots have attracted great attention from the research community given their very attractive luminescent properties. However, the recent discovery that some of these properties may result from fluorescent impurities originating from the synthesis process, and not from the carbon dots themselves, constitute a significant setback to our knowledge of these materials. Herein, we proceeded to the study of carbon dots generated from citric acid and urea *via* a microwave-assisted synthesis, focusing on their analysis by AFM, HR-TEM, XPS, FT-IR, ESI-MS, UV-Vis and fluorescence spectroscopy. We have found that this synthesis process does generate molecular fluorophores that can mask the luminescence of the carbon dots. More importantly, our data demonstrates that when present in the same solution, the carbon dots and these fluorophores do not behave as separated species with individual emission. Instead, they interact to produce a hybrid luminescence, which excited state properties and reactivity are different from the properties of the individual species. These results indicate the possibility for the development of hybrid materials composed by carbon dots and related molecular fluorophores with new and improved properties.

Introduction

Carbon dots (CDs) are carbon-based nanoparticles with a near spherical shape, with a core that might be amorphous or nanocrystalline.[1–3] The core is thought to be composed mostly of graphitic carbon (sp^2 carbon) connected by sp^3 carbon atoms in between.[4,5] On the surface can be found different functional groups (such as carboxylic acids, alcohols and amines), depending on the precursors used and the type of synthetic approach employed.[4,6]

CDs possess an array of desirable properties, such as high photoluminescence,[2,3,7] a broadband optical absorption,[8] biocompability,[4,9] low toxicity,[10] high photostability[6] and chemical stability,[11] and good water solubility.[2,6] Thus, there is no surprise that CDs have gained relevance in several fields, such as in fabrication of light emission devices,[12,13] bioimaging,[14] sensing,[15–17] photocatalysis,[3] drug delivery[18] and photodynamic therapy.[19]

Despite the high number of studies focusing on the characterization of CDs and on the development of new applications for them, the origin of their photoluminescence is still a matter of debate.[7,20] In fact, several models and explanations have been presented so far: quantum confinement effect,[21,22] emission from surface states,[23,24] self-trapped excitons,[25] band gap emission,[21,22] surface dipole emissive centers,[26] and formation of H-aggregate type excitonic states,[27,28] among others.

More recently, there has been an increasing focus on the potential role of molecular fluorophores on the photoluminescence of CDs. It has been demonstrated by several authors that bottom-up synthesis of CDs, arguably the most common route for their fabrication, also produces several molecular by-products.[29–33] More importantly, these by-products were shown to be quite fluorescent. In fact, efficient separation of the CDs and molecular fluorophore fractions revealed the former to be weakly fluorescent and the latter strongly fluorescent.[29–33] This evidence suggest that the fluorescence typically associated with CDs may result instead from these fluorescent impurities, which constitute a significant setback to our knowledge of these nanomaterials.

Given this, it is essential to have a better understanding of the relationship between the fluorescence of the CDs and these fluorescent impurities. More specifically, we intend to understand

[a] Chemistry Research Unit (CIQUP), Faculty of Sciences of University of Porto, R. Campo Alegre 697, 4169-007 Porto, Portugal
[b] X-Ray Photoelectron Spectroscopy Lab, Central Service to Support Research Bulding (SCAI), University of Málaga, 29071 Málaga, Spain
[c] CQM-Centro de Química da Madeira, Universidade da Madeira, Campus da Penteada, 9020-105 Funchal, Portugal
[d] LACOMEPHI, GreenUPorto, Department of Geosciences, Environment and Territorial Planning, Faculty of Sciences of University of Porto, R. Campo Alegre 697, 4169-007 Porto, Portugal. E-mail: luis.silva@fc.up.pt

† Electronic supplementary information (ESI) available: FT-IR spectra, XPS spectra, ESI-MS spectra, fluorescence spectra in different conditions. See DOI: 10.1039/c9cp03730f

if when present in the same solution, the carbon dot and the fluorescent impurities are well separated and behave as individual species with well-defined fluorescent behavior. Or if upon synthesis, the CDs and the fluorescent impurities interact to generate a synergistic effect. It should be noted that has been demonstrated that the fluorescent moiety of the CDs is present inside the nanoparticle in a flexible environment.[34]

While that would not negate the need for a through and efficient sample purification and characterization, if correct the latter hypothesis could lead to future fabrication of hybrid materials with different properties. To this end, we have proceeded to the microwave-assisted treatment of citric acid and urea in aqueous solution. Characterization by AFM, XPS, FT-IR, ESI-MS, UV-Vis and fluorescence spectroscopy revealed the existence of both CDs and fluorescent impurities. Subsequent fractioning of the mixture allowed us to obtain three samples: CDs, the fluorescent impurities, and a mixture containing both the nanoparticle and the fluorescent impurities. Study of the photochemical reactivity of the three samples towards different electron-withdrawing/-donating probes demonstrated that when present in the same solution, the fluorescent impurities and CDs do not present individual photoluminescent properties. On the contrary, they interact to generate synergistic effects, different than their individual responses. This finding indicates that: the efficient purification of CDs samples is required because existent fluorescent impurities not only mask their fluorescent signal, but alter it; there is the potential for the development of carbon dot – molecular fluorophores with hybrid properties.

Experimental methods

Synthesis of carbon dots

CDs were prepared by microwave treatment (5 minutes at 700 W in a domestic microwave) of citric acid (0.5 g) and urea (0.5 g) in aqueous solution (5 mL), which was placed in a glass beaker. In the end, 5 mL of deionized water were used to re-suspend the resulting product, yielding a solution of CDs. This solution was subsequently subjected to centrifugation (10.000 rpm for 10 minutes), being this a common method of removing suspended impurities from the solution of CDs.[15,16] However, centrifugation is not able by itself to separate the CDs from molecular impurities that originate from the bottom-up synthesis. To this end, CDs were further purified by dialysis. This process was carried out using a Float-A-Lyzer®G2 Dialysis Device SPECTRUM® (molecular weight cut-off of ~1000 Da). The dialysis process ran continuously for 3 days with regular changes in the dialysis wash waters.

Samples analysis and characterization

Fluorescence was measured in standard 10 mm fluorescence quartz cells by using a Horiba Jovin Yvon Fluoromax-4 spectrofluorimeter. The spectra were obtained with a 1 nm interval and 5 nm slit widths.

Absorption spectra were obtained with a VWR® UV-3100PC spectrophotometer, by using quartz cells.

FT-IR analysis was performed using a PerkinElmer® Spectrum Two FT-IR spectrometer.

Direct injection ESI-MS was made using a Thermo Finnigan™ LCQ™ Deca XP Max (Thermo Electron Corporation, Waltham, USA) mass spectrometer. This device consists on electrospray interface as ionization source and a quadruple ion trap for MS^n experiments. It was operated as follows: spray voltage, 5 kV; capillary voltage, ±15 V; capillary temperature, 300 °C.

X-ray photoelectron spectroscopy (XPS) measurements were recorded on a Physical Electronic PHI VersaProbe II spectrometer utilizing Al-K_α with a hemispherical multichannel detector (53.6 W, 15 kV and 1486.6 eV). Spectra were recorded using a 200 μm diameter circular analysis area, with a constant pass energy value at 29.35 eV. PHI SmartSoft software was employed for results analysis, further processed using MultiPak Version 9.6 package. Carbon C 1s signal (284.8 eV) was used as reference to determine the binding energy values, using Shirley type background and Gauss–Lorentz curves.

AFM analysis was carried out using a Veeco Metrology Multimode/Nanoscope IVA by tapping. A silica plate was used to deposit the sample for analysis and an AFM RTESP cantilever was used.

Suspensions of nanoparticles were characterized by high-resolution transmission electron microscopy (HR-TEM) and examined under a FEI Talos F200X.

Results and discussion

Given our aim of understanding the possible interactions between CDs and fluorescent impurities resulting from their synthesis, three samples needed to be obtained. One would be a sample where both species co-exist in solution, while the other two would be samples of the individual samples. The first sample is the one that results after centrifugation, now termed $CDs_{centrifuged}$, given that this purification method is only able to eliminate suspended impurities and not low-weight fluorescent compounds.[15,16,29] Individual samples of the CDs and fluorescent impurities were obtained *via* dialysis.[29,33] This process generates two water fractions, one inside and one outside the dialysis bag. The inside fraction consists on high-weight species, which are expected to be the CDs themselves,[29,33] being this sample termed $CDs_{dialyzed}$. The outside fraction consists on low-weight species, which are expected to be the fluorescent impurities,[29,33] being this sample now termed $Water_{FI}$.

The first step of this study was to perform a structural analysis of the CDs, both in the presence ($CDs_{centrifuged}$ sample) and in the absence ($CDs_{dialyzed}$ sample) of fluorescent impurities. The size of the CDs was determined by AFM analysis of the $CDs_{dialyzed}$ sample (Fig. S1, ESI†), which were found to have a size of 23.1 nm. It should be noted that while CDs are typically sized bellow 10 nm, it is not uncommon to find such nanoparticles with bigger sizes (up to 30 nm).[35,36] Nevertheless, the morphology of $CDs_{dialyzed}$ was analysed by HR-TEM microscopy (Fig. 1), showing well dispersed nanoparticles with a medium diameter size of 6.5 nm, with uniform spherical shapes.

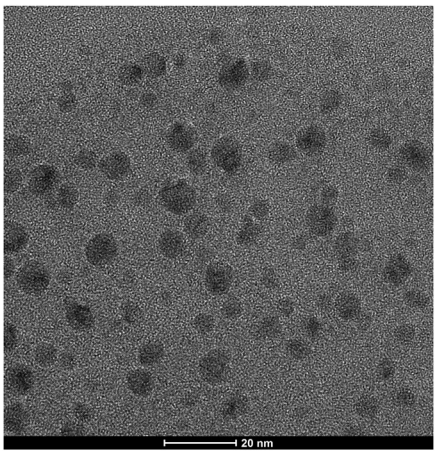

Fig. 1 HR-TEM image for $CDs_{dialyzed}$.

Thus, we can conclude that some aggregation occurred during AFM experiments.

XPS analysis was performed to characterize the surface composition of $CDs_{centrifuged}$ and $CDs_{dialyzed}$ (Fig. S2–S4, ESI†).[37] The XPS mole fraction of $CD_{centrifuged}$ is of 59.70% C, 16.75% N and 23.55% O. A detailed scan for the internal levels of C 1s, O 1s and N 1s was made, towards deconvolution and chemical state and the quantitative analysis. The C 1s splits into three peaks: at binding energies of 284.8 eV (54.53%), 288.3 eV (33.50%) and 286.6 (11.95%). These peaks can be attributed to C–C/C–H/adventitious carbon (284.8 eV), C–O/C–N (286.6–286.9 eV) and C═O/O–C═O carbonyl/carboxylic groups (288.3–288.6 eV), respectively. The core level spectrum of N 1s revealed a dominant peak at 400 eV (88.9%) and a shoulder at 401.5 eV (11.1%). These can be attributed to amine/amide groups and to protonated amines, respectively. Finally, the deconvolution of O 1s spectrum revealed two peaks: a dominant one at 531.5 eV (80.9%) due to C═O linkage; a smaller one at 532.7 eV (18.1%), which results from C–O/C–O–C groups. The results for $CDs_{dialyzed}$ are quite similar, with just a slight increase in the XPS mole fraction of C (from 59.70 to 62.57%), with the subsequent decrease of the mole fractions of N (from 16.75 to 15.47%) and O (from the 23.55 to 21.97%). Thus, these results indicate that the surface composition of the $CDs_{centrifuged}$ and $CDs_{dialyzed}$ are identical, and that purification by dialysis apparently has a limited effect on the CDs sample.

These results are supported by further analysis of the surface functional groups of both $CDs_{centrifuged}$ and $CDs_{dialyzed}$, this time made by FT-IR spectroscopy (Fig. S5, ESI†). FT-IR analysis revealed quite similar spectra for both samples. They show the presence of a band at 3300 cm^{-1}, indicating the presence of O–H/N–H groups. Also, both samples displayed peaks at 1655 cm^{-1} (generally attributed to C═C groups or primary amides), 1575 cm^{-1} (N–H bending vibrations for secondary amides), 1350 cm^{-1} (O–H bending vibrations) and at 1185 cm^{-1} (generally attributed to C–N stretching vibrations from amines).

However, optical analysis does not support this similarity between $CDs_{centrifuged}$ and $CDs_{dialyzed}$. The UV-Vis spectrum of $CD_{dialyzed}$ (Fig. 2A) revealed a main band at 340 nm and a shoulder at 245 nm. These can be attributed to n–π* and π–π* (C═C/C═N bonds) transitions, respectively.[38,39] There is also less well-resolved and small band at 410 nm. By its turn, the UV-Vis spectrum of $CD_{centrifuged}$ presents not just one but two shoulders, at 245 and 275 nm. Furthermore, the band at

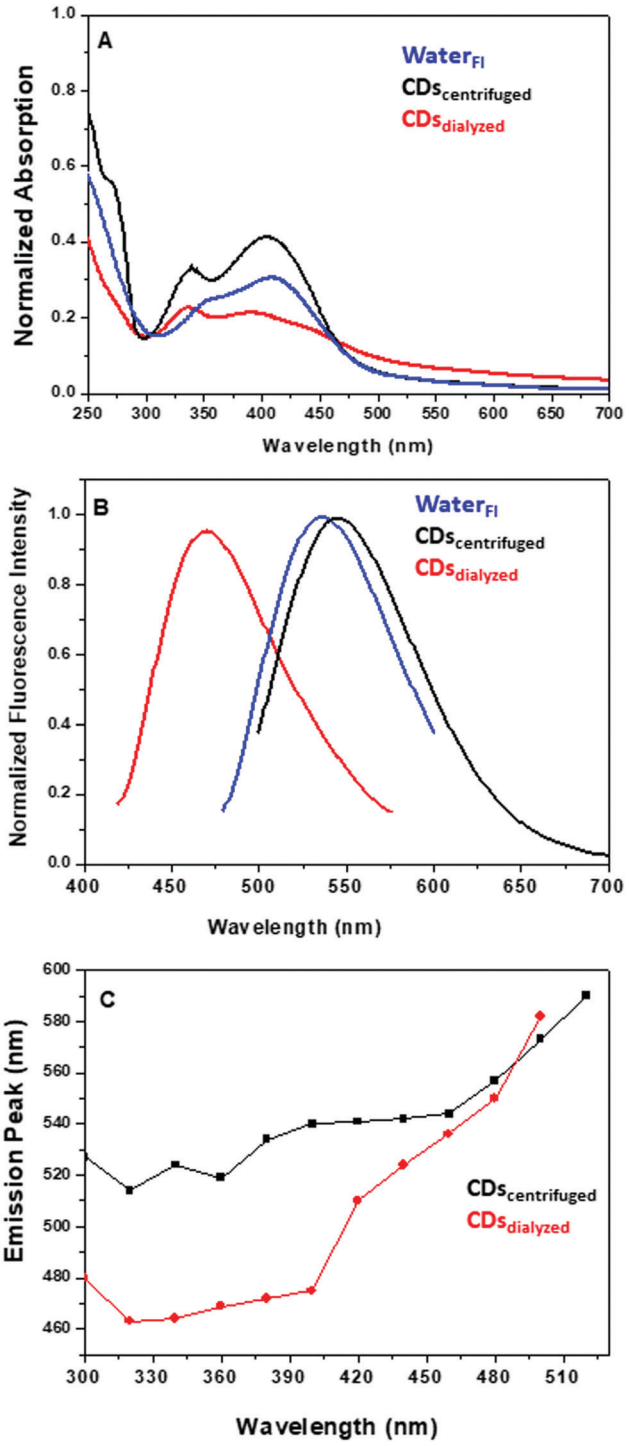

Fig. 2 (A) Normalized UV-Vis spectra for $CDs_{centrifuged}$, $CDS_{dialyzed}$ and $Water_{FI}$; (B) normalized fluorescence spectra for $CDs_{centrifuged}$, $CDS_{dialyzed}$ and $Water_{FI}$. The excitation wavelength maxima used were 410 nm for $CDs_{centrifuged}$ and $Water_{FI}$, and 380 nm for $CDs_{dialyzed}$; (C) emission wavelength as a function of excitation wavelength for $CDs_{centrifuged}$ and $CDs_{dialyzed}$.

410 nm is now well-resolved and is higher than the one at 340 nm. The most significant optical difference between the two CD samples is relative to their emission profiles (Fig. 2B). While the emission maximum of $CD_{centrifuged}$ is at 540 nm, the emission of $CDs_{dialyzed}$ is significantly blue-shifted, with a peak at 475 nm. The excitation wavelength maxima of the samples are also difference, with $CD_{centrifuged}$ being excited at 410 nm and $CDs_{dialyzed}$ being excited at 380 nm. This indicates that purification by dialysis can produce a significant effect on the photoluminescent properties of the CDs samples. Nevertheless, it should be noted that both $CDs_{centrifuged}$ and $CDs_{dialyzed}$ present excitation-dependent emission, with both samples reaching similar emission wavelengths at higher excitation wavelengths (Fig. 2C). It should be noted that what is plotted on Fig. 2C is the centre of the emission peak.

The differences between the optical properties of $CDs_{centrifuged}$ and $CDs_{dialyzed}$ can be attributed to the presence of fluorescent impurities.[29]

In fact, optical analysis by both UV-Vis (Fig. 2A) and fluorescence spectroscopy (Fig. 2B) of the $Water_{FI}$ sample revealed an identical spectrum to $CD_{centrifuged}$, but different from $CD_{dialyzed}$. More specifically, $Water_{FI}$ is also photoexcited at 410 nm and has an emission wavelength maximum at 540 nm, besides presenting a UV-Vis spectrum with the same bands and shoulders as $CDs_{centrifuged}$. Thus, these measurements demonstrate that the optical signals observed from $CDs_{centrifuged}$ result not from the CDs itself, but from lower-weight fluorescent impurities. We have also compared the fluorescence intensity of $CDs_{dialyzed}$, $CDs_{centrifuged}$ and $Water_{FI}$ in aqueous solution (Fig. S6, ESI†), with the same concentration for each sample (1 mg mL^{-1}). These results showed that while $CDs_{centrifuged}$ and $Water_{FI}$ present intensities of the same magnitude, they present intensities 6 and 8 times higher than that presented by $CDs_{dialyzed}$. This is in line with recent literature in which it is indicated that fluorescent impurities are strongly fluorescent, while the CDs are only weakly fluorescent.[29–33] This analysis supports the attribution of the fluorescence emitted by $CDs_{centrifuged}$ to the fluorescent impurities, which mask the signal of the CDs.

Mass spectroscopic analysis was also made by subjecting the $CDs_{centrifuged}$, $CDs_{dialyzed}$ and $Water_{FI}$ to direct-injection ESI-MS. The resulting mass spectra (in the positive and negative ionization modes) can be found on Fig. S7 and S8 (ESI†). In the positive ionization mode (Fig. S7, ESI†), the mass spectrum of $CDs_{centrifuged}$ (scanned between 50.0 m/z and 500.0 m/z) presents three predominant peaks at 173.13 m/z, 190.20 m/z and 397.53 m/z followed by several medium sized ones. However, the mass spectrum of $CD_{dialyzed}$ in positive ionization mode presents just a dominant peak at 397.73 m/z, followed by small peaks at 291.47 m/z and 374.53 m/z. By its turn, the mass spectrum in the positive ionization mode of $Water_{FI}$ is quite like that of $CDs_{centrifuged}$, with the difference of a now reduced contribution by the peak at 397.73 m/z. Similar differences and relationships can be seen on the mass spectra in the negative ionization mode (Fig. S8, ESI†). The mass spectrum of $CDs_{centrifuged}$ is composed by several predominant peaks with m/z lower than 400.0 m/z, and by several moderate peaks in the 350–500 m/z region. By their turn, the mass spectrum of $CDs_{dialyzed}$ is dominated by peaks in the 350–500 m/z region, while the mass spectrum of $Water_{FI}$ has no significant peaks in that region but presents in the same peaks as $CDs_{centrifuged}$ in the 50–350 m/z region.

This analysis is not enough to properly identify the fluorescent impurities (which is outside the scope of this study) but demonstrates that the bottom-up synthesis of CDs does produce a mixture of fluorescent species that needs to be subjected to further purification steps (like dialysis) to separate the lower-weight fluorescent impurities from the desired nanoparticles.[29]

Nevertheless, regarding the possible identity of the fluorescent impurities, we wish to point out that in the negative ionization ESI-MS analysis (Fig. S8, ESI†), the predominant peak for $CDs_{centrifuged}$ and $Water_{FI}$ is at 179.27 m/z. This peak could be attributed to 4-hydroxy-1*H*-pyrrolo[3,4-*c*]pyridine 1,3,6(2*H*,5*H*)-trione (HPPT, mol. wt. of 180 g mol^{-1}), which was identified by Kasprzyk *et al.*[33] as a fluorescent by-product of the microwave-assisted synthesis of CDs. Moreover, HPPT was found to have a bright green emission and an absorption peak at 410 nm, which is in line with the optical properties of $CDs_{centrifuged}$ and $Water_{FI}$ (Fig. 2A and B).[33] Furthermore, the peak at $\sim$179 m/z is not relevant in the mass spectrum of $CDs_{dialyzed}$. Thus, these results point to HPPT being a main responsible for masking the fluorescence of the carbon dot in the $CDs_{centrifuged}$ sample, being removed from the solution after dialysis.

The view that the bottom-up synthesis can generate fluorescent impurities that, if not removed, can mask the signal of the carbon dot was further supported by measuring the fluorescence of the three samples ($CDs_{centrifuged}$, $CDs_{dialyzed}$ and $Water_{FI}$) at different pH values (Fig. S9, ESI†). This was achieved by measuring the fluorescence of these samples in neat water, in aqueous solution acidified with HCl (0.1 M), and in aqueous solution basified with NaOH (0.1 M). As expected, the emission profiles of $CDs_{centrifuged}$ and $Water_{FI}$ are identical in these conditions. Namely, both these samples show a green emission in neat and acidified water, while there is a significantly blue-shift at basic pH. As for $CDs_{dialyzed}$, there are no significant shifts in the emission peak with changes in the pH.

A similar study was made by measuring the fluorescence spectra of $CDs_{centrifuged}$, $CDs_{dialyzed}$ and $Water_{FI}$ in different solvents: methanol (MeOH), acetonitrile (ACN), dimethylformamide (DMF) and dimethyl sulfoxide (DMSO). These results can be found on Fig. 3. Despite their different properties, these solvents had only a negligible effect on the fluorescent spectrum of $CDs_{dialyzed}$. This could point to the fluorescent moieties of $CDs_{dialyzed}$ to be inside the nanoparticle, and so, not exposed to the external microenvironment.[34,40] By its turn, the fluorescent spectra of $Water_{FI}$ undergo relevant blue-shifts when comparing with the 540 nm in aqueous solution: 515 nm in MeOH, 510 nm in ACN, and 500 nm in DMSO and DMF. That would indicate that the fluorescent moieties are exposed to the external medium,[34,40] which indicates a difference between the $Water_{FI}$ and $CDs_{dialyzed}$ samples. Interestingly, the solvents exert a somewhat intermediate effect on $CDs_{centrifuged}$.

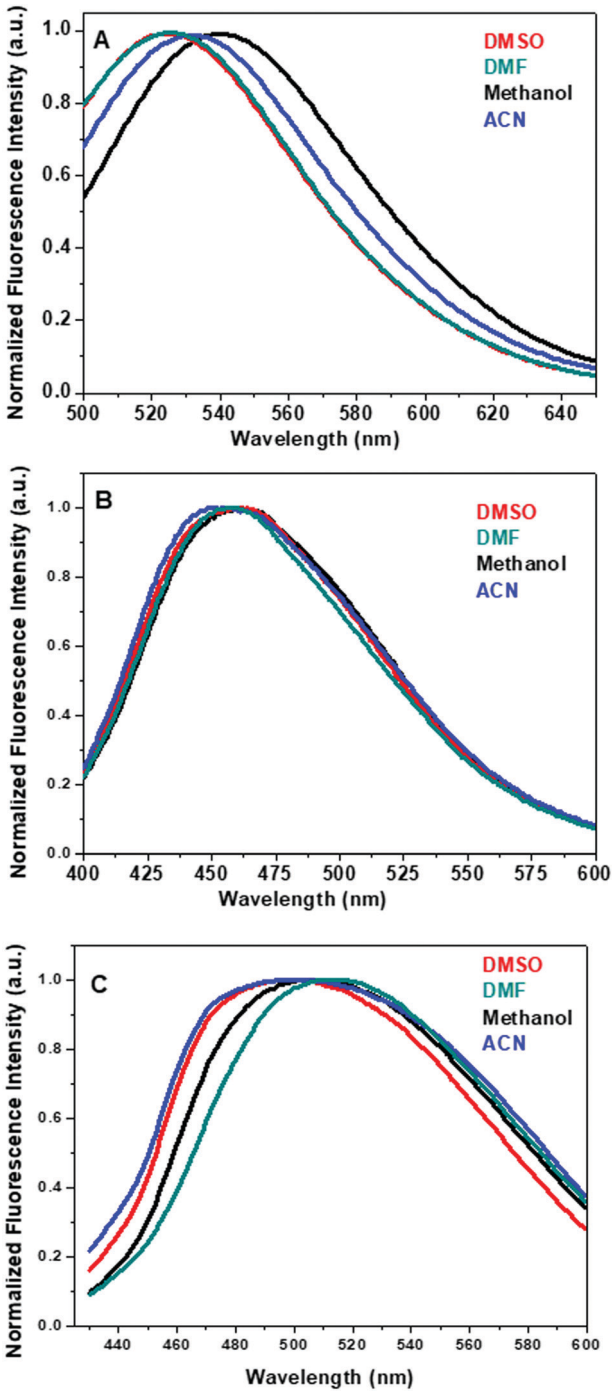

Fig. 3 Normalized emission spectra for $CDs_{centrifuged}$ (a), $CDs_{dialyzed}$ (b) and $Water_{FI}$ (c) in the presence of acetonitrile (ACN), dimethylformamide (DMF), dimethyl sulfoxide (DMSO) and methanol (MeOH).

The solvents do induce a blue-shift to the emission maxima, the same as $Water_{FI}$, but to a lesser extent (between 525 nm and 530 nm). This would indicate that the fluorescent moieties of $CDs_{centrifuged}$ are also exposed to the solvent, the same as $Water_{FI}$. However, the smaller blue-shift indicates that the fluorescent moieties are also more shielded than the moieties present in $Water_{FI}$. Thus, the presence on the nanoparticles on the $CDs_{centrifuged}$ sample affects the fluorescence properties of the fluorescent impurities.

The results obtained so far show that the bottom-up synthesis of the present CDs also generate fluorescent by-products that can mask the fluorescent signal of the nanoparticle itself, which is in line with recent literature.[29–33] However, these results do not indicate if when present in the same solution, the CDs and the fluorescent impurities interact to generate synergistic effects. To this end, we proceeded to study the excited state reactivity of the $CDs_{centrifuged}$, $CDs_{dialyzed}$ and $Water_{FI}$ samples. This was made by measuring the response of the three samples toward electron-donating (diphenylamine) and electron-withdrawing (nitromethane) molecules. By comparing the responses of the individual particles (either $CDs_{dialyzed}$ and $Water_{FI}$) with that of the samples where both co-exist ($CDs_{centrifuged}$), we can assess if the CDs and the fluorescent impurities do interact to generate a different signal than just the one resulting from their individual responses.

The next step of this study was then to assess the photochemical responses of the three samples ($CDs_{centrifuged}$, $CDs_{dialyzed}$ and $Water_{FI}$) toward nitromethane (Fig. 4). This is an electron-withdrawing molecule, and so, can be a useful non-ionic electron-acceptor probe for the study of photoinduced electron transfer (PET) reactions involving the present samples. Nitromethane induces quenching for both samples, indicating that all samples might be capable of PET reactions as an electron-donor. Furthermore, all emission profiles follow a Stern–Volmer relationship. However, nitromethane is a significantly more efficient quencher of $CDs_{dialyzed}$ (Stern–Volmer constant, K_{SV}, of $23.7 \pm 0.1\ \mu M^{-1}$) than of the other samples. Moreover, the K_{SV} for $CDs_{centrifuged}$ ($5.4 \pm 0.2\ \mu M^{-1}$) and $Water_{FI}$ ($6.1 \pm 0.4\ \mu M^{-1}$) are quite similar. Once again indicating that the responses observed for CDs samples only subjected to centrifugation might result only from fluorescent impurities.

We have also analysed the effect exerted by diphenylamine on the fluorescence of $CDs_{centrifuged}$, $CDs_{dialyzed}$ and $Water_{FI}$ (Fig. 5). Diphenylamine is a known redox indicator and a strong electron-donor. Thus, it can also be used to study the potential of the three samples in PET reaction, in this case as electron-acceptors. Given the results so far, we were expecting somewhat different emission profiles between $CDs_{centrifuged}$/$Water_{FI}$ and $CDs_{dialyzed}$. To our surprise, that was not the case. There were indeed observed differences between $CDs_{centrifuged}$ and $CDs_{dialyzed}$.

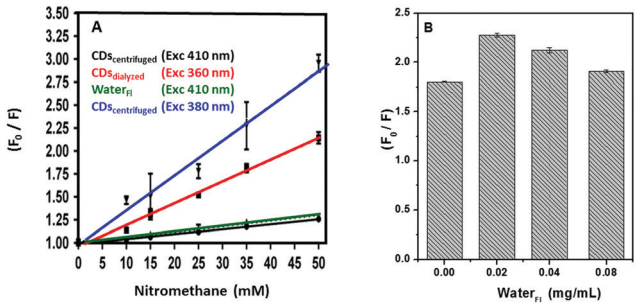

Fig. 4 (a) F_0/F values in the presence of different concentrations of nitromethane (0–50 mM); (b) represents the variation of F_0/F values of $CDs_{dialyzed}$ samples (0.04 mg mL^{-1}) in the presence of nitromethane (45 mM), to which were added different amounts of $Water_{FI}$ (0.02–0.08 mg mL^{-1}).

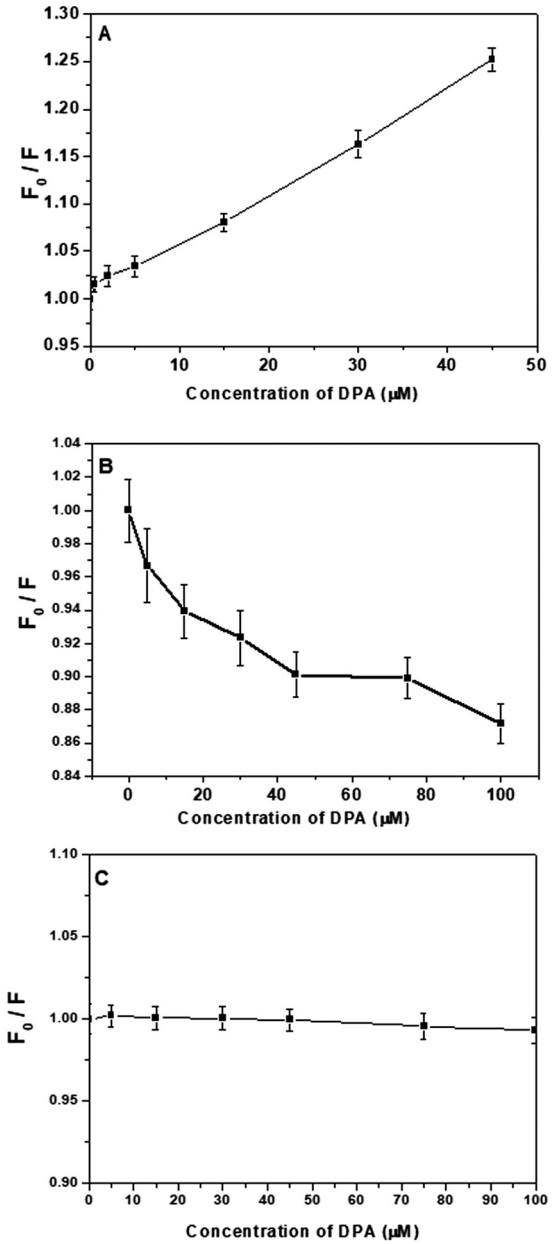

Fig. 5 F_0/F values of $CDs_{centrifuged}$ (a), $CD_{dialyzed}$ (b) and $Water_{FI}$ (c) in the presence of diphenylamine.

The former sample was subjected to quenching induced by diphenylamine that followed a Stern–Volmer relationship (K_{SV} of 0.0054 μM^{-1}). By its turn, diphenylamine induces an opposite effect (fluorescence enhancement) on the emission of $CDs_{dialyzed}$, a difference expected given the findings described above. What surprised us was that diphenylamine had no effect on the fluorescence of $Water_{FI}$. That indicates that the diphenylamine-induced quenching observed for $CDs_{centrifuged}$ did not originate from fluorescent impurities. However, given that diphenylamine only induced fluorescence enhancement for $CDs_{dialyzed}$, that diphenylamine-induced quenching could not have originated from the CDs itself. Thus, this data indicates that when combined in the same solution, the fluorescent impurities and the nanoparticles can interact to generate a synergistic effect. That is, they produce an effect different than the one originating from their separated forms.

A synergistic effect can also be seen if we re-evaluate the results obtained during the nitromethane-related assays (Fig. 4A). More specifically, by using a ~380 nm excitation instead of the excitation maximum of 410 nm, the fluorescence spectra of $CDs_{centrifuged}$ presents a shoulder at ~460 nm, which can be attributed to the emission of the nanoparticle itself (Fig. S10, ESI†). Thus, we have measured the response of $CDs_{centrifuged}$ towards nitromethane by using a ~380 nm excitation, and by measuring the fluorescence intensity at ~460 nm (Fig. 4). This should allow us to monitor the nanoparticles itself but in the presence of fluorescent impurities. The resulting emission profile (Fig. 4A) also shows a significant quenching effect that follows a Stern–Volmer relationship, which indicates a qualitative agreement with the results of $CDs_{dialyzed}$. However, the determined K_{SV} ($38.0 \pm 2.5\ \mu M^{-1}$) was now almost the double of that determined for $CDs_{dialyzed}$ ($23.7 \pm 0.1\ \mu M^{-1}$). Thus, it appears that the presence of fluorescent impurities enhances the nitromethane-related quenching process of the nanoparticle itself. Given that the fluorescent impurities by themselves do not suffer significant quenching (K_{SV} of $6.1 \pm 0.4\ \mu M^{-1}$), this enhancement must result from a synergistic effect between the carbon dot and the fluorescent impurities, and not just from an additive phenomenon.

To assess if the fluorescent impurities can indeed modulate the photochemical reactivity of the CDs, we have measured the response of $CDs_{dialyzed}$ towards nitromethane in the presence of increasing concentrations of $Water_{FI}$ (Fig. 4B). In fact, we can see that addition of fluorescent impurities to $CDs_{dialyzed}$ increases the nitromethane-induced quenching. However, this quenching enhancement decreases with increasing amounts of the impurities. This can be explained as follows: the fluorescent impurities interact with the carbon dot, which leads to the formation of a sort of hybrid material with synergistic properties, such as the enhancement of the nitromethane-induced quenching. Increasing the quantity of the fluorescent impurities to a certain threshold, however, could mask the surface of the carbon dot and prevent its interaction with the quencher. Thereby, offsetting the enhancement effect generated by the fluorescent impurities – carbon dot synergy.

Conclusions

In conclusion, we have characterized the structural and optical properties of citric acid, urea-derived CDs by using a diverse set of experimental techniques: AFM, HR-TEM, XPS, FT-IR, ESI-MS, UV-Vis and steady-state fluorescence spectroscopy. We have demonstrated this microwave-assisted synthesis produces green-emitting molecular fluorophores that can mask the luminescence of the blue-emitting CDs. More importantly, our data show that when present in the same solution, these fluorophores and the carbon dots do not behave as separated species with individual emission. Instead, they interact to

generate a hybrid luminescence, which excited state properties and reactivity are different than just the sum of their individual properties. These results indicate the possibility for the development of hybrid materials composed by CDs and related molecular fluorophores with improved properties.

Conflicts of interest

There are no conflicts to declare.

Acknowledgements

This work was made in the framework Sustainable Advanced Materials (NORTE-01-00145-FEDER-000028), funded by ''Fundo Europeu de Desenvolvimento Regional (FEDER)'', through ''Programa Operacional do Norte'' (NORTE2020). Acknowledgment to projects POCI-01-0145-FEDER-006980, PTDC/QEQ-QFI/0289/2014 and PTDC/QEQ-QAN/5955/2014 are also acknowledged. The first project is funded by FEDER through COMPETE2020, while the latter two are co-funded by FCT/MEC (PIDDAC) and by FEDER through COMPETE-POFC. Luís Pinto da Silva acknowledges funding from FCT under the Scientific Employment Stimulus (CEECIND/01425/2017). The Laboratory for Computational Modelling of Environmental Pollutans-Human Interactions (LACOMEPHI) is acknowledged. D. M. A. C. acknowledges FCT for funding relative to her PhD grant (SFRH/BD/144423/2019). This work was supported by FCT-Fundação para a Ciência e a Tecnologia (projectPEst-OE/QUI/UI0674/2019, CQM, Portuguese Government funds), and through Madeira 14-20 Program, project PROEQUIPRAM – Reforço do Investimento em Equipamentos e Infraestruturas Científicas na RAM (M1420-01-0145-FEDER-000008) and by ARDITI-Agência Regional para o Desenvolvimento da Investigação Tecnologia e Inovação, through the project M1420-01-0145-FEDER-000005 – Centro de Química da Madeira – CQM+ (Madeira 14-20). We thank *Centro de Materiais da Universidade do Porto* (CEMUP) for performing the AFM measurements (www.cemup.up.pt).

Notes and references

1 K. Hola, Y. Zhang, Y. Wang, E. P. Giannelis, R. Zboril and A. L. Rogach, *Nano Today*, 2014, **9**, 590–603.
2 J. C. G. Esteves da Silva and H. M. R. Gonçalves, *Trends Anal. Chem.*, 2011, **30**, 1327–1336.
3 R. Wang, K.-Q. Lu, Z.-R. Tang and Y.-J. Xu, *J. Mater. Chem. A*, 2017, **5**, 3717–3734.
4 S. N. Baker and G. A. Baker, *Angew. Chem., Int. Ed.*, 2010, **49**, 6726–6744.
5 A. P. Demchenko and M. O. Dekaliuk, *Methods Appl. Fluoresc.*, 2013, **1**, 042001.
6 S. Y. Lim, W. Shen and Z. Gao, *Chem. Soc. Rev.*, 2015, **44**, 362–381.
7 Y. Xiong, J. Schneider, E. V. Ushakova and A. L. Rogach, *Nano Today*, 2018, **23**, 124–139.
8 Z. Peng, X. Han, S. Li, A. O. Al-Youbi, A. S. Bashammakh, M. S. El-Shahawi and R. M. Leblanc, *Coord. Chem. Rev.*, 2017, **343**, 256–277.
9 Y. P. Sun, B. Zhou, Y. Lin, W. Wang, K. A. Fernando, P. Pathak, M. J. Meziani, B. A. Harruff, X. Wang, H. Wang, P. G. Luo, H. Yang, M. E. Kose, B. Chen, L. M. Veca and S. Y. Xie, *J. Am. Chem. Soc.*, 2006, **128**, 7756–7757.
10 K. Wang, Z. Gao, G. Gao, Y. Wo, Y. Wang, G. Shen and D. Cui, *Nanoscale Res. Lett.*, 2013, **8**, 122.
11 O. Kozák, K. K. R. Datta, M. Greplová, V. Ranc, J. Kašlík and R. Zbořil, *J. Phys. Chem. C*, 2013, **117**, 24991–24996.
12 J. Joseph and A. A. Anappara, *ChemPhysChem*, 2017, **18**, 292–298.
13 Y. Zhou, P. Y. Liyanage, D. L. Geleroff, Z. Peng, K. J. Mintz, S. D. Hettiarachchi, R. R. Pandey, C. C. Chusuei, P. L. Blackwelder and R. M. Leblanc, *ChemPhysChem*, 2018, **19**, 2589–2597.
14 Y. F. Kang, Y. H. Li, Y. W. Fang, Y. Xu, X. M. Wei and X. B. Yin, *Sci. Rep.*, 2015, **5**, 11835.
15 D. M. A. Crista, G. P. C. Mello, O. Shevchuk, R. M. S. Sendao, E. F. C. Simoes, J. M. M. Leitao, L. P. da Silva and J. C. G. Esteves da Silva, *J. Fluoresc.*, 2019, **29**, 265–270.
16 E. F. C. Simões, J. M. M. Leitão and J. C. G. E. da Silva, *Microchim. Acta*, 2016, **183**, 1769–1777.
17 C. L. Shen, L. X. Su, J. H. Zang, X. J. Li, Q. Lou and C. X. Shan, *Nanoscale Res. Lett.*, 2017, **12**, 447.
18 S. D. Hettiarachchi, R. M. Graham, K. J. Mintz, Y. Zhou, S. Vanni, Z. Peng and R. M. Leblanc, *Nanoscale*, 2019, **11**, 6192–6205.
19 H. He, X. Zheng, S. Liu, M. Zheng, Z. Xie, Y. Wang, M. Yu and X. Shuai, *Nanoscale*, 2018, **10**, 10991–10998.
20 M. K. Barman and A. Patra, *J. Photochem. Photobiol., C*, 2018, **37**, 1–22.
21 K. Jiang, S. Sun, L. Zhang, Y. Lu, A. Wu, C. Cai and H. Lin, *Angew. Chem., Int. Ed.*, 2015, **54**, 5360–5363.
22 F. Yuan, Z. Wang, X. Li, Y. Li, Z. Tan, L. Fan and S. Yang, *Adv. Mater.*, 2017, **29**, 1702910.
23 L. Tang, R. Ji, X. Cao, J. Lin, H. Jiang, X. Li, K. S. Teng, C. M. Luk, S. Zeng, J. Hao and S. P. Lau, *ACS Nano*, 2012, **6**, 5102–5110.
24 L. Bao, C. Liu, Z. L. Zhang and D. W. Pang, *Adv. Mater.*, 2015, **27**, 1663–1667.
25 L. Xiao, Y. Wang, Y. Huang, T. Wong and H. Sun, *Nanoscale*, 2017, **9**, 12637–12646.
26 S. Ghosh, A. M. Chizhik, N. Karedla, M. O. Dekaliuk, I. Gregor, H. Schuhmann, M. Seibt, K. Bodensiek, I. A. Schaap, O. Schulz, A. P. Demchenko, J. Enderlein and A. I. Chizhik, *Nano Lett.*, 2014, **14**, 5656–5661.
27 A. P. Demchenko and M. O. Dekaliuk, *Nanoscale*, 2016, **8**, 14057–14069.
28 M. O. Dekaliuk, O. Viagin, Y. V. Malyukin and A. P. Demchenko, *Phys. Chem. Chem. Phys.*, 2014, **16**, 16075–16084.
29 J. B. Essner, J. A. Kist, L. Polo-Parada and G. A. Baker, *Chem. Mater.*, 2018, **30**, 1878–1887.
30 Y. Song, S. Zhu, S. Zhang, Y. Fu, L. Wang, X. Zhao and B. Yang, *J. Mater. Chem. C*, 2015, **3**, 5976–5984.
31 J. Schneider, C. J. Reckmeier, Y. Xiong, M. von Seckendorff, A. S. Susha, P. Kasák and A. L. Rogach, *J. Phys. Chem. C*, 2017, **121**, 2014–2022.

32 L. Shi, J. H. Yang, H. B. Zeng, Y. M. Chen, S. C. Yang, C. Wu, H. Zeng, O. Yoshihito and Q. Zhang, *Nanoscale*, 2016, **8**, 14374–14378.
33 W. Kasprzyk, T. Swiergosz, S. Bednarz, K. Walas, N. V. Bashmakova and D. Bogdal, *Nanoscale*, 2018, **10**, 13889–13894.
34 A. Das, D. Roy, C. K. De and P. K. Mandal, *Phys. Chem. Chem. Phys.*, 2018, **20**, 2251–2259.
35 Y. Liang, H. Zhang, Y. Zhang and F. Chen, *Anal. Methods*, 2015, **7**, 7540–7547.
36 S. Tao, Y. Song, S. Zhu, J. Shao and B. Yang, *Polymer*, 2017, **116**, 472–478.
37 B. B. Campos, C. Abellan, M. Zougagh, J. Jimenez-Jimenez, E. Rodriguez-Castellon, J. C. Esteves da Silva, A. Rios and M. Algarra, *J. Colloid Interface Sci.*, 2015, **458**, 209–216.
38 A. Sharma, T. Gadly, A. Gupta, A. Ballal, S. K. Ghosh and M. Kumbhakar, *J. Phys. Chem. Lett.*, 2016, **7**, 3695–3702.
39 W. Wang, B. Wang, H. Embrechts, C. Damm, A. Cadranel, V. Strauss, M. Distaso, V. Hinterberger, D. M. Guldi and W. Peukert, *RSC Adv.*, 2017, **7**, 24771–24780.
40 J. Ren, F. Weber, F. Weigert, Y. Wang, S. Choudhury, J. Xiao, I. Lauermann, U. Resch-Genger, A. Bande and T. Petit, *Nanoscale*, 2019, **11**, 2056–2064.

